JOURNAL OF MATERIALS SCIENCE: MATERIALS IN MEDICINE 9 (1998) 159–163

Sol–gel derived porous hydroxyapatite coatings

WENJIAN WENG
Department of Materials Science and Engineering, Zhejiang University, Hangzhou 310027, People's Republic of China

J. L. BAPTISTA
Department of Ceramics and Glass Engineering, University of Aveiro, Aveiro 3810, Portugal

The preparation of hydroxyapatite coatings on alumina substrates by a sol–gel method was investigated. A mixed ethanol solution of $Ca(NO_3)_2 \cdot 4H_2O$ and P_2O_5 was used as a dipping source. The samples were characterized by solid-state ^{31}P nuclear magnetic resonance spectroscopy, differential thermal analysis, thermogravimetry, X-ray diffraction, scanning electron microscopy and infrared reflection spectroscopy. The coating obtained at 500 °C had good hydroxyapatite crystallinity, adhesive strength of about 10 MPa and dense morphology. The coating obtained at 750 °C also had good crystallinity and adhesive strength but porous morphology. © *1998 Chapman & Hall*

1. Introduction

Hydroxyapatite (HAP) is an important ceramic material in the replacement of hard tissues, because it can form a strong bond with the bone through inducing bone formation [1]. However, the mechanical properties of HAP ceramics are not good enough to be used as an implant subjected to a load [2]. If HAP is produced in the form of coatings, its advantages can be very properly taken. The experimental results have shown that the fixation between the bone tissues and implants such as titanium alloy and alumina can be improved through HAP coatings [3].

There are a number of methods for producing HAP coatings, as reviewed by Lacefield [4]. The most popular one at present is a plasma-spraying process, whereby the coating is formed when HAP ceramic particles are propelled through a high-temperature (10 000–30 000 °C) plasma zone and fused together upon striking the surfaces of implants [5–7]. Because HAP is not stable at a high temperature, plasma-sprayed HAP coatings usually contain calcium oxide, tricalcium phosphate, tetracalcium phosphate and other calcium phosphate phases [8]. In addition, using the plasma-spraying method, it seems difficult to produce a porous coating which can greatly enhance an establishment of the strong bonding between implants and the bone [9].

A sol–gel method has been proved to prepare coatings at relative low temperatures with a capability of tailoring their morphologies and compositions [10]. Attempts to prepare HAP coatings by the sol–gel method or a similar way have been reported [11, 12]. However, these did not seem to be very successful because of the selected dipping sources which caused the formation of HAP only at a high temperature (1100 °C) and with a low adhesive strength of the coatings. The purpose of this work was to prepare HAP coatings by the sol–gel method using a mixed ethanol solution of $Ca(NO_3)_2 \cdot 4H_2O$ and P_2O_5 as a dipping source. The formation process of the HAP phase and the HAP coatings in this way was investigated and discussed.

2. Experimental procedure

The procedure for the synthesis of 2M ethanol solution of P_2O_5 was described previously [13]. 4M ethanol solution of $Ca(NO_3)_2 \cdot 4H_2O$ was prepared before mixing. A mixed ethanol solution of $Ca(NO_3)_2 \cdot 4H_2O$ and P_2O_5 in a Ca/P ratio of 1.67 was refluxed for 24 h. All chemical reagents used in this work were Guarantee Reagent (G, R) level. In order to understand the formation process of HAP phase from the dipping solution, the solution was transformed to powders by pouring it on to a hot stainless steel plate at about 150 °C. Then, the as-prepared powders were calcined at 500 and 750 °C, respectively.

For the preparation of HAP coatings on alumina substrates (Hoechst Ceram Tec AG), a liquid coating was formed by a dipping method using the mixed solution. The substrates were dipped into the solution and withdrawn at a rate of 4 cm min^{-1}. The as-dipped liquid coatings were dried at 150 °C for about 15 min and the dried coatings were heated at 500 °C for 10 min for each run. In order to increase the thickness of the coatings, ten runs were performed. Some of the as-prepared coatings were further heated at 500 °C for 12 or 24 h, some were further heated at 750 °C for 0.5 h.

In this work, the ^{31}P solid-state nuclear magnetic resonance (NMR) spectrum was measured in a Fourier transform NMR spectrometer (Bruker MSL 400P) at 161.978 MHz with a magic-angle spinning and recycle delays of 60 s, and the chemical shifts were noted (p.p.m.) from H_3PO_4 (aq. 85 wt %); differential thermal analysis (DTA) and thermogravimetric analysis (TG) curves were recorded in a thermal analyser

(Type LCP-1, Beijing Optical Device Co.) with a heating rate of 10 °C min^{-1}. X-ray diffraction (XRD) patterns were obtained in an X-ray powder diffractometer (Rigaku, D/MAX-B) with a step size of 0.05° and a scan speed of 2.00° min^{-1}; IR reflection spectra were scanned in a Fourier transform–infrared reflection spectrometer (Mattson Glaxy 7020) with resolution of 4 cm^{-1}; and morphological observations of coatings were done in a scanning electron microscope (Hitachi, S-4100).

The adhesive strength of the coatings was measured according to a method described elsewhere [14]. A superglue (Permatex®) was used. Three runs were done for each sample.

3. Results

3.1. ^{31}P solid NMR spectrum

The ^{31}P solid-state NMR spectrum (Fig. 1) of the as-prepared powders mainly consists of peaks at 2.97, −0.97, −4.35, −7.50 and −10.25 p.p.m., respectively. However, the spectrum of the powders calcined at 500 °C has one peak at 2.67 p.p.m. (Fig. 1).

3.2. DTA and TG curves

In the DTA and TG curves (Fig. 2), there is a big endothermic peak at 160 °C with a 25% weight loss, two exothermic peaks at 270 °C with 12% weight loss and at 420 °C with 10% weight loss, respectively. After 500 °C, the curves have no obvious changes.

3.3. XRD patterns

The XRD patterns in Fig. 3 show that the as-prepared powders have $Ca(NO_3)_2$ crystalline phase and a small amount of HAP phase. The powders calcined at 500 °C have HAP phase. The powders calcined at 750 °C have HAP phase with minor β-TCP phase, and the HAP phase develops somewhat better because it has a smaller half-peak width of 0.29° at (2 1 1) than that of 0.34° for the powders heated at 500 °C.

For the coatings on alumina substrates, the as-prepared coating and the coating heated at 750 °C have HAP phase (Fig. 4). In addition, the relative XRD intensity of $I_{HAP(211)}/I_{\alpha\text{-}Al_2O_3(012)}$ increases from 0.21 for the as-prepared coating to 0.34 for the coating heated at 750 °C. For the coatings heated at 500 °C, the $I_{HAP(211)}/I_{\alpha\text{-}Al_2O_3(012)}$ intensity in the coatings increases with heating times. This value is 0.21, 0.32 and 0.33 for the as-prepared coating and coatings heated for 12 and 24 h, respectively.

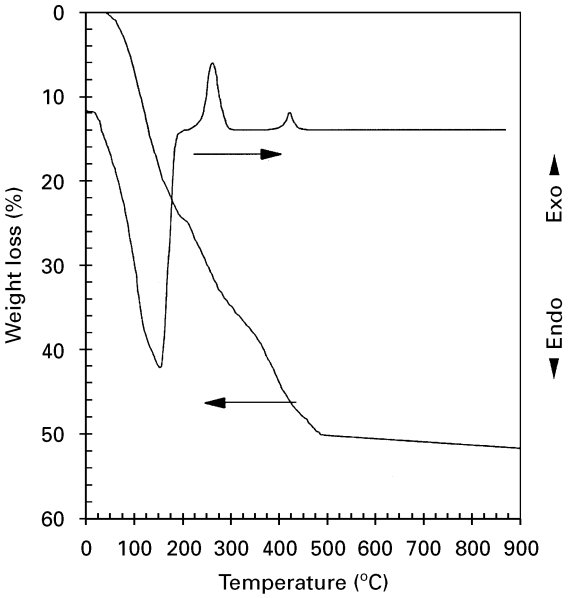

Figure 2 DTA and TG curves of the as-prepared powders.

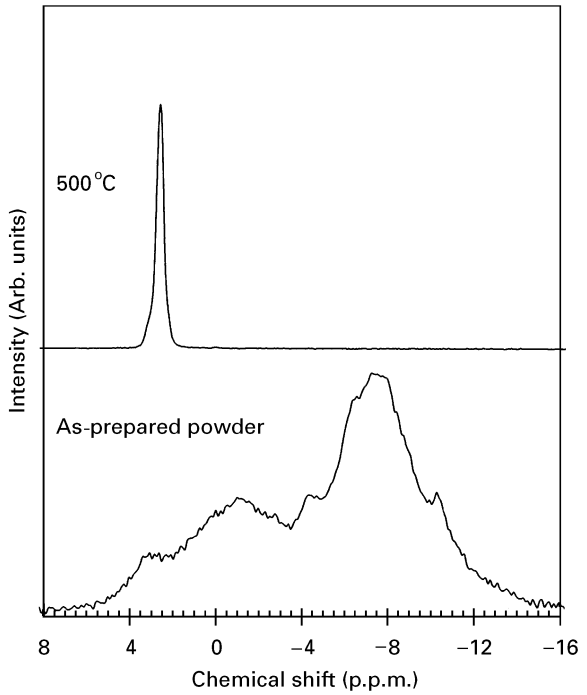

Figure 1 Solid-state ^{31}P NMR spectra of the as-prepared powders and the powders heated at 750 °C.

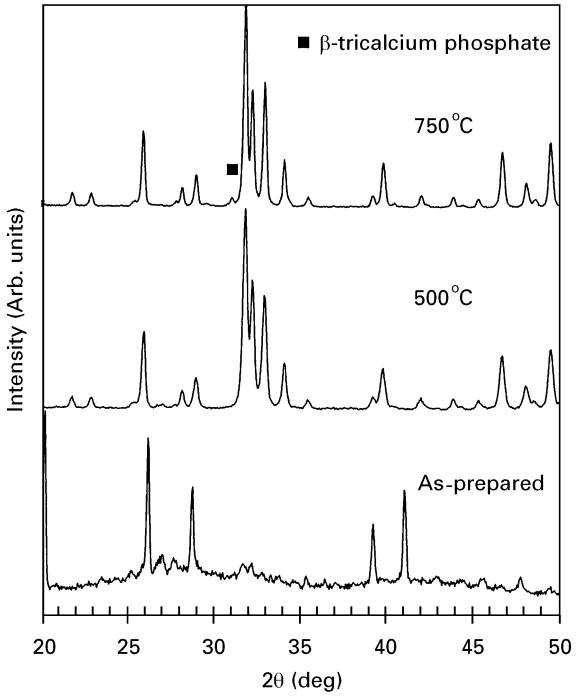

Figure 3 The XRD patterns of the as-prepared powders and the powders heated at 500 and 750 °C.

3.4. SEM observations

The as-prepared coating is dense as shown in Fig. 5a and b, in which the grains are difficult to identify. The coating heated at 750 °C is porous as shown in Fig. 5c and d in which the HAP grain size is found to be about 0.1 μm and the grains have a very good connection. The as-prepared coating has a thickness of about 2 μm.

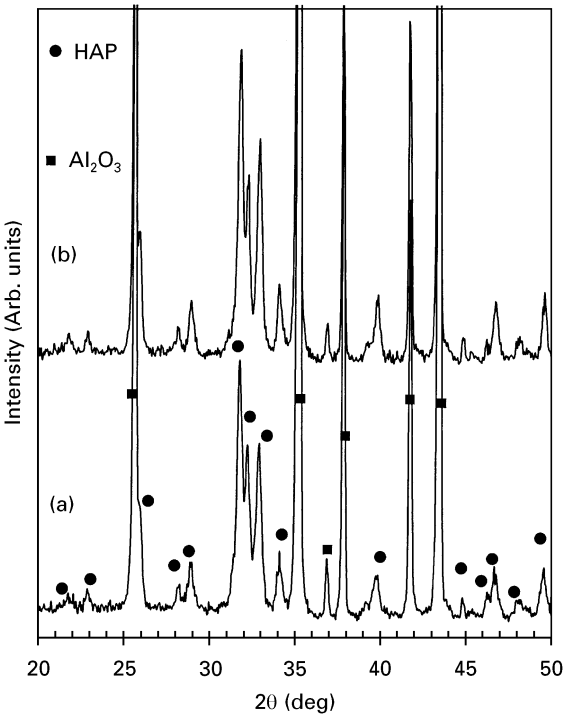

Figure 4 The XRD patterns of the (a) as-prepared coating and (b) the coating heated at 750 °C.

3.5. IR reflection spectra

In the high wave number range, the IR reflection spectra (Fig. 6) show a band of OH groups at 3571 cm^{-1} for the as-prepared coating and the coating heated at 750 °C. In the middle wave number range, there is a band of CO_3^{2-} groups at 1460 cm^{-1} only for the as-prepared coatings, and a wide and strong band contributed by the substrate for both coatings (Fig. 6). In the low wave number range (Fig. 7), there are the bands related to PO_4^{3-} groups and OH groups although these spectral profiles are different from those of absorption spectra of HAP powders [15], which could be due to the influence of the very strong band of the substrate. The significant bands are a well-split band of OH groups at 630 cm^{-1} for both coatings, and a band of CO_3^{2-} groups at 850 cm^{-1} for the as-prepared coating.

3.6. The adhesive strength

The adhesive strength of the as-prepared coating and the coating heated at 750 °C has no obvious differences and is 10.5 ± 1.4 MPa.

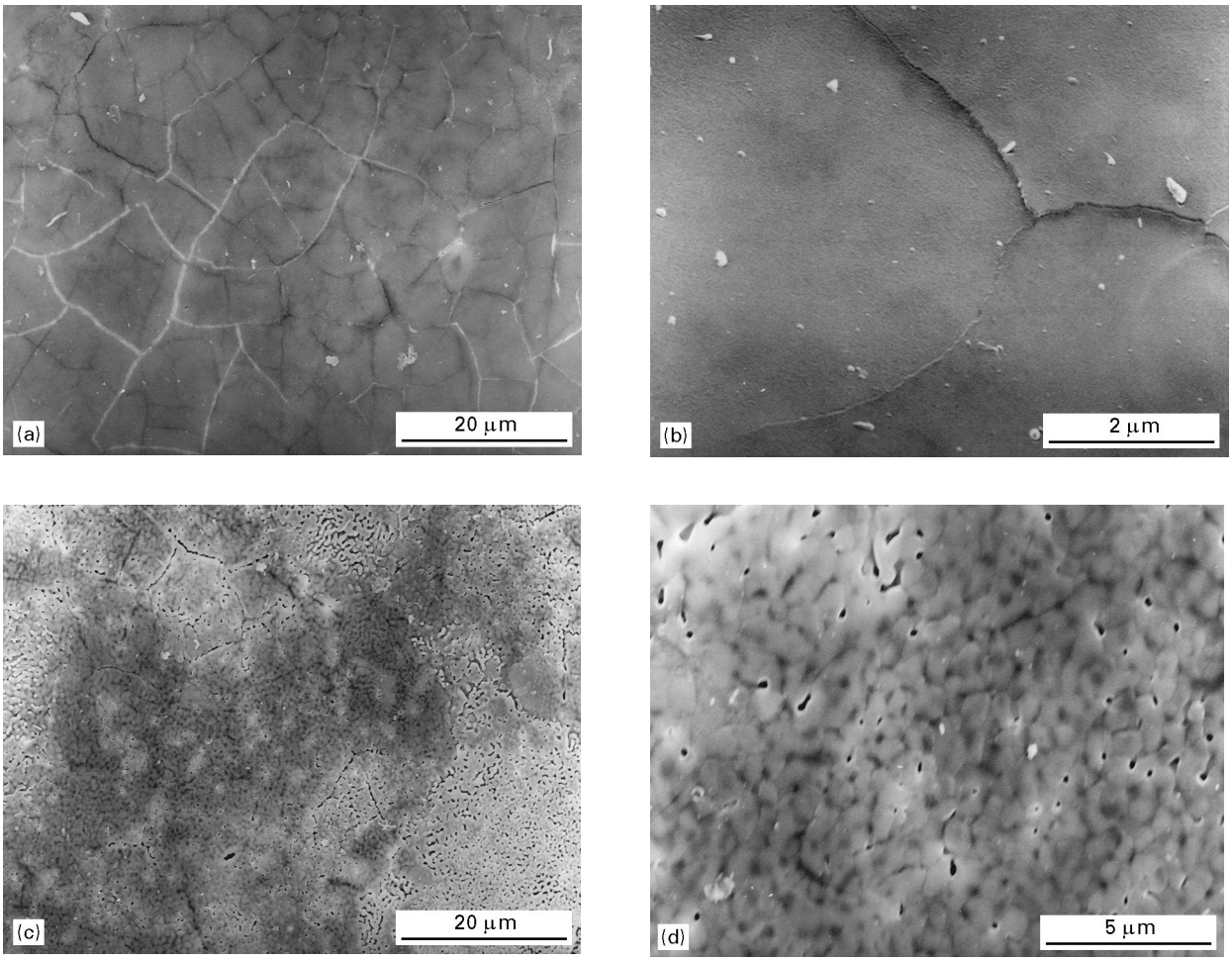

Figure 5 Scanning electron micrographs of (a, b) the as-prepared coating; (c, d) the coating heated at 750 °C.

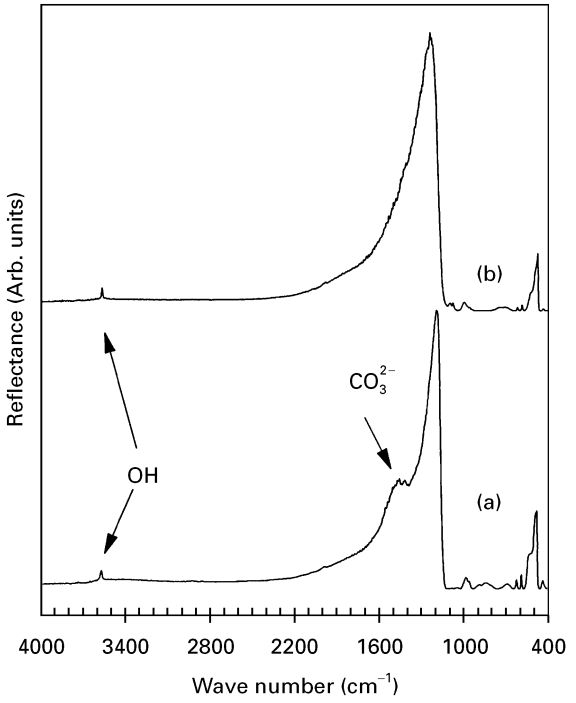

Figure 6 The IR reflection spectra of (a) the as-prepared coating and (b) the coating heated at 750 °C in the full wave number range.

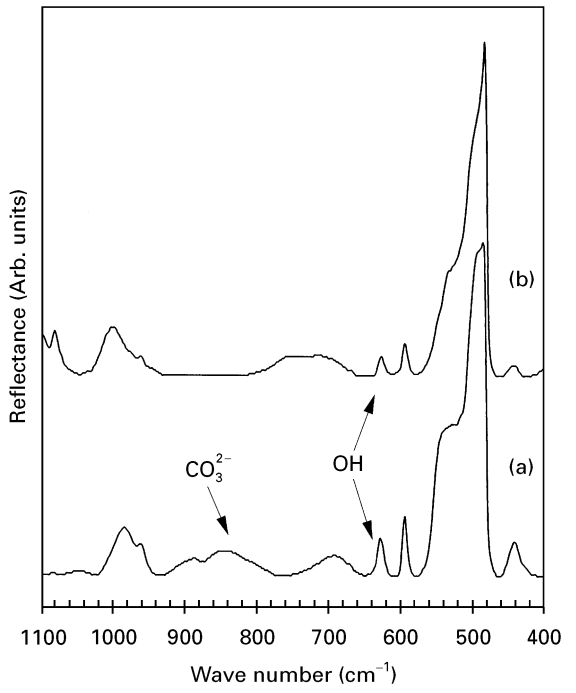

Figure 7 The IR reflection spectra of (a) the as-prepared coating and (b) the coating heated at 750 °C in the wave number range from 400–1100 cm^{-1}.

4. Discussion

In the as-prepared powders obtained from the mixed solution of $Ca(NO_3)_2 \cdot 4H_2O$ and P_2O_5, the two precursors have not completely reacted to form calcium phosphates because of the presence of calcium nitrate crystallites (Fig. 3). The incomplete consumption of calcium nitrate is attributed to not very reactivity of OEt groups in the phosphorus precursor [16].

The TG curve (Fig. 2) shows that the as-prepared powders have totally a 51% weight loss. One-half of the weight loss is contributed by the evaporation because the powders are very hygroscopic, another half arises from the decomposition and burn-out of the nitrate and OEt groups based on the DTA curve (Fig. 2). The latter weight loss implies that the as-prepared powders contain a certain amount of OEt groups. In addition, the final hydroxyapatite formation on calcining (Fig. 3) also gives a sign that the as-prepared powders have the phosphorus species with OH groups. Hence, the as-prepared powders could be considered to be a mixture of calcium nitrate, hydroxyapatite and $x\mathrm{CaO} \cdot y[\mathrm{PO}_{m+1}(\mathrm{OH})_n(\mathrm{OEt})_o]$ with different values of x, y, m, n, and o ($2m + n + o = 3$), although the compositions cannot be accurately identified in this work. In the as-prepared powders, hydroxyapatite leads to a peak at 2.98 p.p.m., and $x\mathrm{CaO} \cdot y[\mathrm{PO}_{m+1}(\mathrm{OH})_n(\mathrm{OEt})_o]$ species lead to peaks at -0.97, -4.35, -7.50 and -10.25 p.p.m. in the NMR spectrum (Fig. 1).

The direct transformation of the as-prepared powders to a pure HAP phase (Figs 1 and 3) at a moderate temperature of 500 °C indicates that the as-prepared powders have a reasonably good homogeneity. The further increase in heat-treatment temperatures favours the development of the HAP phase and induces the formation of a small amount of β-TCP (Fig. 3). The formation of β-TCP could be attributed to the HAP powders obtained at 500 °C containing a small amount of a poorly developed carbonated HAP phase (Fig. 6a) which was decomposed at 750 °C.

For the coatings, the HAP formation process is the same as that in the form of powders except no β-TCP in the coating heated at 750 °C. No appearance of β-TCP in the XRD pattern (Fig. 4b) of the coating heated at 750 °C could be because the amount of β-TCP in the coating is too small to detect for the XRD measurement. The as-prepared coating has a reasonably good HAP crystallinity and contains some carbonated HAP according to the XRD pattern (Fig. 4a) and IR spectra (Figs 6a and 7a) in which there is the sharp band at 3571 cm^{-1} and a well-split band at 630 cm^{-1} related to OH groups, and the bands at 1460 and 850 cm^{-1} related to CO_3^{2-} groups. When the heat-treatment time at 500 °C is prolonged, the coating heated for 12 h has a better developed HAP phase, and the further extension of the duration has no obvious effects on the development. When the as-prepared coating is heated at 750 °C, the HAP develops better too. The further development of the HAP in the as-prepared coating by prolonging heat-treatment time or increasing heat-treatment temperature could be due to the coarsening of the HAP grains as shown in Fig. 5c and d. The coarsening process of the HAP grains also leads to the formation of porosity in the coating as compared with the dense morphology of the as-prepared coating (Fig. 5a and b). Based on Fig. 5d, the porosity of the coating heated at 750 °C is approximately estimated to be 30 vol % by a stereographic method [17].

The adhesive strength of the HAP coatings has a reasonably good value of about 10 MPa. This value could result from the good connection between the coatings and the substrates and among the grains

in the coatings. No obvious effect of further increase in heating temperature on the adhesive strength could be attributed to the good bonding which was obtained between the coating and the substrate at 500 °C.

The present method seems versatile to prepare the HAP coatings with or without carbonated HAP, with porous or dense morphology, with good adhesive strength and crystallinity and with moderate preparation temperatures. These should favour applications *in vivo*.

5. Conclusion

Hydroxyapatite coatings on alumina substrates can be prepared by a mixed solution of $Ca(NO_3)_2 \cdot 4H_2O$ and P_2O_5 through a sol–gel method. The coatings obtained in this work show good HAP crystallinity and adhesive strength. The present method could control the porosity and crystallinity of the HAP coatings by changing the preparation conditions.

Acknowledgement

W. Weng acknowledges the support of the University of Aveiro, the Foundation of the State Education Commission of China, Cao Guangbiao's Foundation of the High-Tech Development of Zhejiang University. He also thanks Dr Panjian Li for many suggestions and help during the work.

References

1. K. DE GROOT, *Biomaterials* **1** (1980) 47.
2. M. SHIRKHANZADEH, *J. Mater. Sci. Mater. Med.* **6** (1995) 90.
3. K. DE GROOT, *J. Ceram. Soc. Jpn* **99** (1991) 943.
4. W. R. LACEFIELD, in "Materials Characteristics versus *in Vivo* Behavior," Vol. 523, edited by P. Ducheyne and J. E. Lemons (Annals of the New York Academy of Sciences, New York, 1988) pp. 72–80.
5. K. DE GROOT, R. GEESINK, C. P. A. T. KLEIN and P. SEREKIAN, *J. Biomed. Mater. Res.* **21** (1987) 1375.
6. C. C. BERNDT, G. N. HADDAD, A. J. D. FARMER and K. A. GROSS, *Mater. Forum* **14** (1990) 161.
7. J. G. C. WOLKER, J. M. A. DE BLIECK-HOGERVORST, W. J. A. DHERT, C. P. A. T. KLEIN and K. DE GROOT, *J. Therm. Spray Technol.* **1** (1992) 75.
8. K. DE GROOT, C. P. A. T. KLEIN, J. G. C. WOLKER and J. M. A. DE BLIECK-HOGERVORST, in "Handbook of Bioactive Ceramics", Vol. 2, edited by T. Yamamuro (CRC Press, Boca Raton, FL, 1990) pp. 132–42.
9. E. C. SHORS and R. E. HOLMES, in "An introduction to bioceramics", edited by L. L. Hench and J. Wilson (World Scientific, London, 1993) pp. 181–98.
10. C. J. BRINKER and G. W. SCHERER, "Sol–gel Science: the physics and chemistry of sol–gel processing" (Academic Press, New York, 1992) pp. 841–53.
11. D. B. HADDOW, P. F. JAMES and R. VAN NOORT, *J. Mater. Sci. Mater. Med.* **7** (1996) 255.
12. T. BRENDEL, A. ENGEL and C. RUSSEL, *ibid.* **3** (1992) 175.
13. W. WENG and J. L. BAPTISTA, *J. Eur. Ceram. Soc.* **17** (1997) 1151.
14. M. T. TANAHASHI, T. YAO, T. KOKUBO, M. MINODA, T. MIYAMOTO, T. NAKAMURA and T. YAMAMURO, *J. Am. Ceram. Soc.* **77** (1994) 2805.
15. K. ISHIKAWA, P. DUCHEYNE and S. RADIN, *J. Mater. Sci. Mater. Med.* **4** (1993) 165.
16. C. SCHMUTZ, P. BARBOUX, F. RIBOT, F. TAULELLE, M. VERDAGUER and C. FERNANDEZ-LORENZO, *J. Non-Cryst. Solids* **170** (1994) 250.
17. W. MAO and X. ZHAO, "Recrystallization and grain growth of metals" (Metallurgical Industry Press, Beijing, 1994) p. 246.

Received 27 November 1996
and accepted 1 September 1997